ELSEVIER

Journal of Non-Crystalline Solids 216 (1997) 124–128

JOURNAL OF NON-CRYSTALLINE SOLIDS

Section 4. Optical fibers

Influence of the cladding thickness on the evolution of the NBOHC band in optical fibers exposed to gamma radiations

O. Deparis [a,b,*], D.L. Griscom [c], P. Mégret [b], M. Decréton [a], M. Blondel [b]

[a] *SCK · CEN, Nuclear Research Centre, 200 Boeretang, B-2400 Mol, Belgium*
[b] *Faculté Polytechnique de Mons, 31 boulevard Dolez, B-7000, Belgium*
[c] *Naval Research Laboratory, Washington, DC 20375, USA*

Abstract

The gamma radiation induced loss spectra are recorded from 400 nm to 700 nm in high OH undoped silica core multimode step-index fibers having thin or thick cladding and polyimide or acrylate coating. For both coating materials, the better radiation resistance of thin-cladding fibers is observed. This behavior was reported in the past but not explained. A physical explanation is proposed on the basis of the assumed existence of peroxy-linkage precursors of the non-bridging oxygen hole centers (NBOHCS) and on the basis of a diffusion-limited radiation hardening due to radiolytic hydrogen released by the coating. Besides the radiation effects, an in-situ heating of the fibers performed after irradiation reveals a sensitivity of microbending losses to temperature. © 1997 Elsevier Science B.V.

1. Introduction

In the past, gamma radiation-induced loss in-situ measurements, performed at 850 nm and room temperature, reported that the smaller the cladding to core diameter ratio (CCDR) the better the radiation resistance of pure silica core multimode step-index (MMSI) fibers at doses up to 1 kGy [1]. In addition, polyimide-coated fibers were found to be more radiation-resistant than acrylate-coated fibers, having the same CCDR [1]. The present work was undertaken to determine whether or not analogies exist between the influences of coating material and CCDR previously observed at 850 nm and the possible effects of these parameters on losses induced in the visible range by doses of the order of 1 MGy or higher. In this paper, the influences of CCDR and coating material are studied by means of gamma radiation-induced loss in-situ measurements from 400 nm to 700 nm (visible range) obtained on the same types of fibre as Ref. [1]. The temperature influence on microbending losses is also studied through a post-irradiation temperature cycle at 80°C (20°C above the test temperature). This influence was mentioned in [1] but not observed, probably because of the lower temperature of the test and the larger bending radius of the fibre coils. Finally, a new model for the recovery of the radiation induced loss at 600 nm is presented and discussed.

* Corresponding author. Present address: Faculté Polytechnique de Mons, 31 boulevard Dolez, B-7000 Mons, Belgium. Tel.: +32-65 374 194; fax: +32-65 374 199; e-mail: deparis@fpms.fpms.ac.be.

PII S0022-3093(97)00123-3

2. Experimental conditions

Two gamma irradiations of optical fibers were carried in the spent fuel facility of SCK · CEN in Mol (Belgium). These irradiations were separated by a 3 day recovery period. The spectra of the, radiation-induced loss were recorded in situ in the visible and near infrared ranges, using an experimental set-up described in Fig. 1. Basically, it uses a white light source (1 to 10 nW output power level in 10 nm bandwidth in the visible range), optical couplers, short reference fibre lengths (not exposed to radiations), an optical switching system and an optical spectrum analyzer [2]. The sensitivity limit of the measurement was 3 dB/m (in the visible range) and the accuracy was ± 0.05 dB/m.

The sample length of each test fibre exposed to radiation was about 10 m and it was wound on a small diameter coil (54 mm). The induced loss is computed as in Ref. [2], following a formula which can be found in Ref. [3]. The temperature was always kept at 60°C, except for a 29 h period (80°C) during the first recovery. The dose rate, measured for each fibre with Perpex dosimeters, was between 5.0 ± 0.1 kGy/h and 5.7 ± 0.1 kGy/h depending on the fibre position in the facility. Final dose achieved was between 1.54 MGy and 1.77 MGy. The four optical fibers under test were all multimode step-index (MMSI) fibers having an undoped silica core and a fluorine-doped silica cladding. They were drawn from Suprasil® F-100 preforms which have large OH (600–800 ppm) and small-Cl (100–125 ppm) contents in the core.

The fibers differed in their cladding to core diameter ratios (CCDR) and their coating material (cfr. Table 1). The drawing speed for acrylate-coated fibers (A1 and A2) was faster than for polyin-tide coated fibers (P1 and P2). Fibers A1 and P1 (same preform) have a thin cladding while fibers A2 and P2 (same preform) have a thick cladding.

Table 1
High-OH pure-silica-core optical fibers under test

Fibre	CCDR (100 μm core diameter)	Coating material	Coating diameter (μm)
P1	1.1	Polyimide	125
P2	1.4	Polyimide	170
A1	1.1	Aerylate	250
A2	1.4	Aerylate	250

3. Results

For three dose values, the spectra of the radiation-induced loss in a thin clad fibre (A1) and in a thick clad fibre (A2) are shown in Fig. 2 and Fig. 3 during the first and the second irradiations, respectively. Similar behaviors were found from the spectra recorded in P1 and P2 fibers (not shown).

In both fibers, the induced absorption band at 600 nm is attributed to the NBOHCs (non bridging oxygen hole centers) [4] while band arising from the ultraviolet and tailing in the visible is attributed to radiolytic chlorine Cl^0 that absorbs light in the near UV region [5]. The evolutions of the radiation-induced loss at 600 mn are shown in Fig. 4 during the

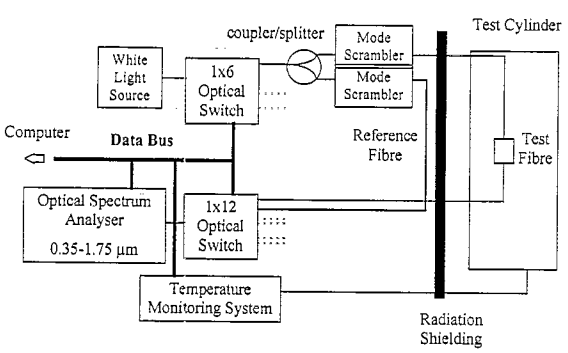

Fig. 1. The experimental set-up for measuring the radiation-induced spectral attenuation [2].

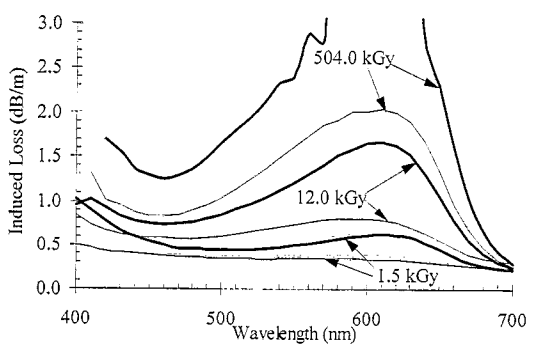

Fig. 2. Spectra of the radiation-induced loss in a thick clad fibre (A2-thick lines) and in a thin clad fibre (A1-thin lines) recorded during the first irradiation.

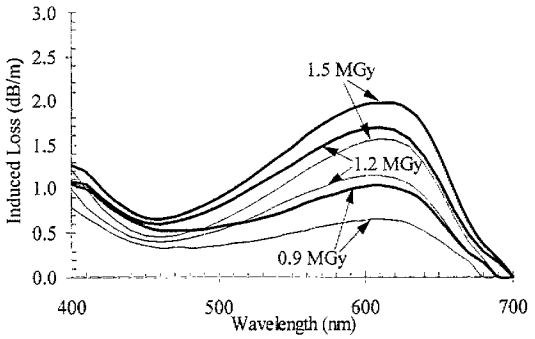

Fig. 3. Spectra of the radiation-induced loss in the same fibers as those of Fig. 2 recorded during the second irradiation.

two irradiation-recovery cycles for the four fibers of this study. In fibers A1 and P1, the saturation of induced loss with increasing dose is already taking place during the first irradiation. The induced loss data obtained during irradiation, $q(D)$, are fitted an *empirical growth model* (inspired from Ref. [6]) given by

$$q(D) = C(1 - e^{-(D/D_{sat})^{\beta}}), \quad (1)$$

where D is the dose and D_{sat}, C and β are the parameters of the model. An example of such a fit is shown in Fig. 4 (triangles, chart 1) for fibre A1 during the first irradiation ($\beta = 0.39$, $D_{sat} = 0.14$ MGy, $C = 2.5$ dB/m). Compared to other models (e.g., $q = CD^{f}$), this model is able to take saturation into account (D_{sat} is called the saturation dose). Note that $D = \dot{D}t$, where t is time and $\dot{D}$ is the dose rate. Therefore, $D_{sat} = \dot{D}\tau_s$, where τ_s can be interpreted as a decay time constant.

In the next section (Section 4), we assume that radiation-hardening takes place due to radiolytic atomic and molecular hydrogen (H^0 and H_2) released by the coating material during irradiation, which diffuses toward the core/cladding interface where it reacts with NBOHCs to form hydroxyl groups. Knowing that any species diffusing through a planar barrier advances as the square root of the time, the rate equation for the decay of NBOHC defects at the core/cladding interface is approximated by a *first order kinetic* with a *time-dependent decay rate* proportional to the square root of the time.

This time dependence is chosen to approximate the amount of free hydrogen at the core/cladding interface as a function of time. To fit the post-irradiation induced loss data, $q(t)$, we thus propose a *compressed exponential recovery model*, given by

$$q(t) = q_0 e^{-t/\tau_0} e^{-(t/\tau)^{3/2}}, \quad (2)$$

where t is the recovery time and q_0, τ, and τ_0 are the parameters of the model. Eq. (2) derives from the

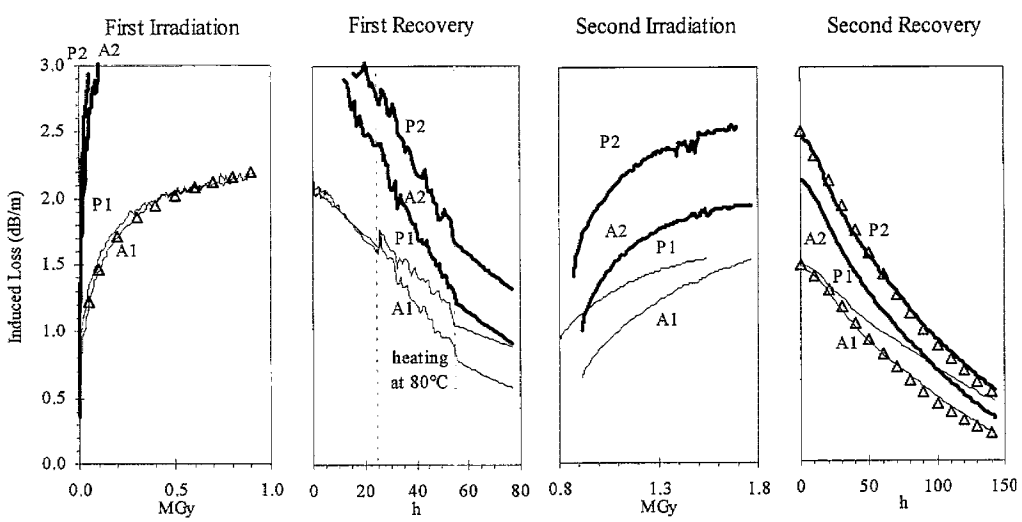

Fig. 4. Evolutions of the radiation-induced loss at 600 nm in the four fibers of this study (cfr. Table 1). Triangles in 1st and 4th charts are computed values for the growth and recovery models (see text).

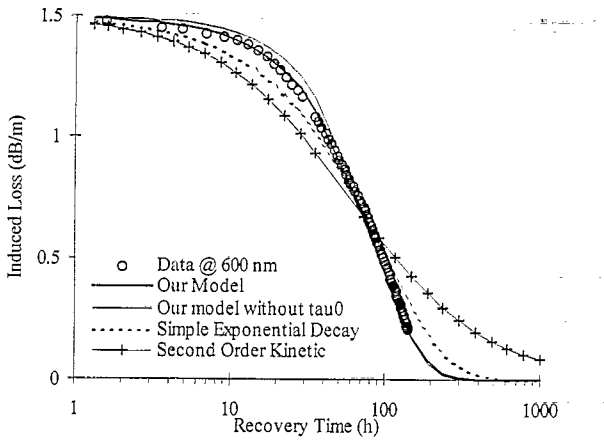

Fig. 5. Comparison of recovery models in the case of fibre A1 during the 2nd recovery (for all models $q_0 = 1.5$ dB/m, for our model, see Eq. (2), $\tau = 104.5$ h and $\tau_0 = 358.4$ h).

postulated first order rate equation with its time-dependent decay rate, $R(t)$, being proportional to the square root of the time

$$\frac{dq(t)}{dt} = -R(t)q(t) = -\left[\frac{1}{\tau_0} + \frac{3}{2\tau}\left(\frac{t}{\tau}\right)^{1/2}\right]q(t). \quad (3)$$

Here, a time-independent term, $1/\tau_0$, has been added to account for decay processes due to hydrogen which has already arrived at the core/cladding interface by the end of the irradiation.

Comparison with other models (e.g., Eq. (2) without the τ_0 term, a simple exponential and a second order decay) shows that our model gives the best fit for all the fibers of this study (see Fig. 5, only the case of fibre A1 is shown here).

In principle, if hydrogen hardening effect is at work, the parameters of Eq. (2) should be related to those of Eq. (1) but we do not yet know how to solve this case exactly. It is supposed that $\tau_s = D_{sat}/\dot{D}$ in Eq. (1) only approximates the kinetics parameterized by τ_0 and τ in Eqs. (2) and (3).

4. Discussion

The spectra (Figs. 2 and 3) as well as the evolution at 600 mn (Fig. 4) of the radiation-induced loss show that both acrylate-coated and polyimide-coated fibers having a thin cladding are more radiation-resistant than those having a thick cladding, especially during the first irradiation. This conclusion was reported in the past [1]. However, no explanation was given for this behavior.

To get an insight into this aspect, it is useful to consider the three mechanisms proposed [7] for the formation NBOHCs (≡Si–O·): namely, the radiolysis of an hydrogen atom from a OH group (≡Si–OH), the breaking of a peroxy linkage (≡Si–O–O–Si≡) and the breaking of a ≡Si–O–Si≡ *stressed* linkage (e.g., stressed by the drawing process). The OH content and the drawing speed being the same, the numbers of precursor of the first and third types might be similar in thin and thick cladding fibers having the same coating material (fibers A1 and A2). Therefore, the observed difference between their radiation response should be due to the second type of precursor. Recently, it has been suggested [8] that peroxy linkages could be created in high-OH silicas *near the core / cladding interface* during the plasma deposition of the F-doped cladding material, following the reaction

$$\equiv Si - OH\,HO - Si\equiv + 2F \rightarrow \equiv Si - O - O - Si\equiv + 2HF\uparrow. \quad (4)$$

The deposition time being longer for obtaining thick cladding fibers, one can reasonably think that, if the above reaction occurs, more peroxy precursors should be created during the fabrication process compared to the case of thin cladding fibers. This might explain the more intense NBHOC band observed in the former compared to the latter, at least during the first irradiation (Fig. 2).

On the other hand, the diffusion of radiolytic hydrogen (H^0 and/or H_2) released by the coating material was recently suggested to explain the annealing of NBOHCs during and after irradiation in plastic coated fibers [9]. This hypothesis was based on the decrease of induced 600 nm NBOHC bands in pure-silica-core acrylate-coated fibers even during irradiation [8] while these fibers were immersed in water. This observed radiation-hardening of plastic-coated fibers must be contrasted with the case of similarly irradiated metal-coated fibers [2,9] wherein the induced NBOHC bands did not saturate at dose of 1.2×10^7 Gy (Si) and did not decay by more than

≈ 10% during a 400 h recovery period [9]. Under the proposed hydrogen hardening mechanism, we guess that a thin clad fibre would en more rapidly than an equivalent thick clad one. However, from curve fitting of the second-cycle recovery data it is found that the decay time constants for the thin and thick clad fibers are virtually identical. This result is interpreted as meaning that the radiolytic hydrogen originating within (or outside) the coating material must traverse the thickness of the cladding rapidly (probably as H^0) *during* irradiation. There it begins to react with the NBOHCs which are known to be concentrated near the core/cladding interface [10]. Following cessation of irradiation, any remaining H^0 probably dimerizes within seconds, so that the ensuing thermal bleaching kinetics are determined by the H_2 already accumulated in the cladding diffusively transporting to the core/cladding interface. Any such H_2 can be expected to react with the NBOHCs and eliminate them [11].

A last thing to be discussed are the fluctuations of induced loss during the post-irradiation temporary heating from 60°C to 80°C (Fig. 4, chart 2). Data recorded in the infrared (not shown here) reveal an *increase* of the induced loss strongly correlated to the temperature elevation, especially in the case of fibre P1. Similar thermal tests performed on virgin samples (unirradiated) of the same fibers than those of this study, confirm that this apparent enhancement of the induced loss during the heating is actually due to microbending losses induced by the thermal expansion of the aluminum spools on which the fibers are wound [2].

5. Conclusion

Our experiment confirms a previously reported observation: the smaller the cladding to core diameter ratio the better the gamma radiation resistance of pure silica core multimode step-index fibers. For the first time, our knowledge, an explanation of this behavior is proposed on the basis of the non-bridging oxygen hole centers (NBOHCs) and on the basis of their annealing through in-diffusion of radiolytic hydrogen released by the coating material. On one hand, we suggest that, at the stage of the preform fabrication, more peroxy precursors of NBOHCs should be created during the deposition of a thick cladding compared to the case of a thin cladding. The very good fits of the recovery data at 600 nm obtained for the fibers of this study provide support for our inference of a radiation-hardening mechanism due to hydrogen released by the coating and diffusing toward the core/cladding interface. This diffusion-limited process could explain, for another part, the better radiation-resistance of thin clad fibers. We also found that for a same core/cladding ratio, the acrylate-coated fibers are about a factor of 2 more radiation-resistant at 600 nm than the polyimide coated fibers. A larger reservoir of radiolytically releasable hydrogen in the much thicker acrylate coatings could explain the superior performance of the acrylate-coated fibers.

References

[1] R.A. Greenwell, C.E. Bames, G.W. Nelson, SPIE 867 (1987) 10.
[2] O. Deparis, P. Mégret, M. Decréton, M. Blondel, IEEE Trans. Nucl. Sci. (Dec. 1996), to be published.
[3] O. Deparis, P. Mégret, M. Decréton, M. Blondel, Proc. RADECS'95 (1995) 507.
[4] K. Nagasawa, Y. Hoshi, Y. Ohki, K. Yahagi, Jpn. J. Appl. Phys. 25 (1986) 464.
[5] K. Nagasawa, M. Tanabe, K. Yahagi, Jpn. J. Appl. Phys. 23 (1984) 1608.
[6] V.A. Mashov, W.R. Austin, L. Zhang, R.G. Leisure, Phys. Rev. Lett. 76 (1996) 2926.
[7] H. Hayami, T. Akutsu, T. Ishitani, K. Suzuki, J. Nucl. Sci. Tech. 30 (1993) 95.
[8] D.L. Griscom, J. Appl. Phys. 77 (1995) 5008.
[9] D.L. Griscom, J. Appl. Phys. 80 (1996) 2142.
[10] K. Nagasawa, R. Tohmon, Y. Ohki, Jpn. J. Appl. Phys. 26 (1987) 148.
[11] D.L. Griscom, J. Non-Cryst. Solids 68 (1984) 301.